

The low temperature limit of the excitonic Mott density in GaN: an experimental reassessment

Léo Mallet-Dida, Pierre Disseix, François Réveret, François Médard, Blandine Alloing, Jesús Zúñiga-Pérez, Joël Leymarie

▶ **To cite this version:**

Léo Mallet-Dida, Pierre Disseix, François Réveret, François Médard, Blandine Alloing, et al.. The low temperature limit of the excitonic Mott density in GaN: an experimental reassessment. New Journal of Physics, 2022, 24, pp.033031. 10.1088/1367-2630/ac58b9 . hal-03617195

HAL Id: hal-03617195
https://cnrs.hal.science/hal-03617195

Submitted on 23 Mar 2022

HAL is a multi-disciplinary open access archive for the deposit and dissemination of scientific research documents, whether they are published or not. The documents may come from teaching and research institutions in France or abroad, or from public or private research centers.

L'archive ouverte pluridisciplinaire **HAL**, est destinée au dépôt et à la diffusion de documents scientifiques de niveau recherche, publiés ou non, émanant des établissements d'enseignement et de recherche français ou étrangers, des laboratoires publics ou privés.

New Journal of Physics
The open access journal at the forefront of physics

Deutsche Physikalische Gesellschaft DPG IOP Institute of Physics

PAPER • OPEN ACCESS

The low temperature limit of the excitonic Mott density in GaN: an experimental reassessment

To cite this article: Léo Mallet-Dida *et al* 2022 *New J. Phys.* **24** 033031

View the article online for updates and enhancements.

You may also like

- Mott transitions with partially filled correlated orbitals
A. Amaricci, L. de' Medici and M. Capone
- Centre of mass motion and the Mott transition in light nuclei
Arij Abdul-Rahman, Mahmoud Alstaty and H R Jaqaman
- Mott transition of excitons in GaAs-GaAlAs quantum wells
G Manzke, D Semkat and H Stolz

This content was downloaded from IP address 195.220.191.133 on 23/03/2022 at 10:51

New Journal of Physics
The open access journal at the forefront of physics

Deutsche Physikalische Gesellschaft DPG
IOP Institute of Physics

Published in partnership with: Deutsche Physikalische Gesellschaft and the Institute of Physics



OPEN ACCESS

RECEIVED
21 December 2021

REVISED
23 February 2022

ACCEPTED FOR PUBLICATION
25 February 2022

PUBLISHED
22 March 2022

Original content from this work may be used under the terms of the Creative Commons Attribution 4.0 licence.

Any further distribution of this work must maintain attribution to the author(s) and the title of the work, journal citation and DOI.



PAPER

The low temperature limit of the excitonic Mott density in GaN: an experimental reassessment

Léo Mallet-Dida[1,*], Pierre Disseix[1], François Réveret[1], François Médard[1], Blandine Alloing[2], Jesús Zúñiga-Pérez[2] and Joël Leymarie[1]

[1] Université Clermont Auvergne, CNRS, Clermont Auvergne INP, Institut Pascal, F-63000 Clermont-Ferrand, France
[2] Centre de Recherche sur l'Hétéro-Epitaxie et ses Applications (CRHEA), Centre National de la Recherche, Rue Bernard Grégory, Sophia-Antipolis, 06560 Valbonne, France
[*] Author to whom any correspondence should be addressed.

E-mail: leo.mallet-dida@doctorant.uca.fr

Keywords: excitonic Mott transition, semiconductors, GaN, spectroscopy, time-resolved photoluminescence, photo-carrier generation, cryogenic temperature

Abstract

The research on GaN lasers aims for a continuous reduction of the lasing threshold. An approach to achieve it consists in exploiting stimulated polariton scattering. This mechanism, and the associated polariton lasers, requires an in-depth knowledge of the GaN excitonic properties, as polaritons result from the coupling of excitons with photons. Under high excitation intensities, exciton states no longer exist due to the Coulomb screening by free carriers; this phenomenon occurs at the so-called Mott density. The aim of this work is to study the bleaching of excitons under a quasi-continuous optical excitation in a bulk GaN sample of high quality through power dependent micro-photoluminescence and time-resolved experiments at 5 K. Time-resolved photoluminescence allows to measure the carrier lifetime as a function of excitation intensity, which is required for a reliable evaluation of the injected carrier density. The vanishing of excitonic lines together with the red-shift of the main emission evidences the occurrence of the Mott transition for a carrier concentration of $(6 \pm 3) \times 10^{16}$ cm^{-3}. This value is more than an order of magnitude smaller than previous determinations published in the literature and is in accordance with many-body calculations.

1. Introduction

Interest in nitride-based semiconductors for optoelectronics has constantly grown over the years. This success is due to the remarkable properties of the material: (i) direct bandgap structure used for optical devices based on (Al, In, Ga)N alloys, which allows for a spectrum of applications from visible to ultraviolet in emission and detection [1]; (ii) significant excitonic binding energies and oscillator strengths, leading to a relative robustness of excitons at high temperature [2]; (iii) well controlled doping and growth [3]. The fabrication of devices such as light emitting diodes and lasers have made it the first III–V material in terms of industrial share in a wide range of wavelengths (white, green, blue, and ultra-violet).

In the context of coherent light emission from GaN-based devices, a potential way to reduce the laser threshold is to use exciton–polaritons within the strong light–matter coupling regime [4]. Exciton–polaritons result from the strong coupling between the first excited states of solids (excitons) and photons. Due to their bosonic character, a gain mechanism based on stimulated relaxation by final-state occupation can trigger polariton condensation and, thus, coherent light emission, at particle densities below those conventionally encountered in edge-emitting and vertical-cavity surface emitting lasers [5].

The research on GaN lasers, and in particular on polariton lasers, requires an in-depth and reliable knowledge of the GaN electronic properties: as excitons may have a substantial role in lowering the laser threshold, it is thus essential to investigate the conditions, in terms of particle density and temperature, under which GaN excitons can exist. This will in turn determine the possible laser gain mechanisms in play

© 2022 The Author(s). Published by IOP Publishing Ltd on behalf of the Institute of Physics and Deutsche Physikalische Gesellschaft

Table 1. Overview of experimental and theoretical Mott densities at low lattice temperatures equal or smaller than 10 K. Estimations of Mott densities obtained from the data provided by each source.

Experimental, in cm^{-3}	Reference
2.2×10^{19}	Hess [11]
6×10^{18}–5×10^{19}	Khym [12]
1×10^{18}	Fischer [13]
1.8–3.8×10^{18}	Binet [14]
6×10^{16}	Present work

that, from a general point of view, may involve polaritonic relaxation stimulated by the final state occupation [5], P-band exciton interactions scattering processes [6], or standard degenerate electron–hole plasma [7].

Excitons in wide bandgap semiconductors have a significant binding energy and are predominant in the near band edge optical response at low temperature and low carrier density [8].

However, with the increase of the excitation density several competing many-body effects need to be taken into account, as large exciton or electron–hole densities reveal the composite nature of excitons. Coulomb exchange interaction and band filling, arising from the Pauli exclusion principle, lead to a lowering of the overall electrostatic energy and a blueshift of the excitonic transition energy. Secondly, the screening of the Coulomb interaction results in a bandgap red-shift and a decrease of both exciton binding energy and oscillator strength. In the case of a 3D material with non-resonant excitation, the screening of the Coulomb interaction is the most efficient effect and the bandgap shift induced by the screening compensates nearly exactly the reduction of the exciton binding energy [9]. Therefore, it is observed that the exciton transition energy remains locked for densities ranging from zero up to the Mott density. The oscillator strength decreases progressively and excitons are dissociated into an electron–hole plasma [10]. This phenomenon referred as the Mott transition is not abrupt and depends upon the temperature. At the critical Mott density, excitons are no longer present in the material.

Table 1 summarizes the experimental values of the Mott densities reported in the literature for GaN with lattice temperatures lower than 10 K [11–14]. The reported data for GaN Mott transitions varies from 1×10^{18} to 5×10^{19} cm^{-3}. The value obtained from the current experiments is also indicated.

It is interesting to establish a comparison between ZnO and GaN experimental values, as a scaling law between those two materials can be established thanks to their excitonic Bohr radii. Versteegh *et al* have carefully studied the exciton screening in ZnO at 300 K through pump-probe reflectivity measurements [15]. In order to obtain an homogeneous carrier density within the penetration of the reflected probe, they induced in the material a three-photon absorption with the 800 nm laser pulses of a Ti-sapphire laser. The Mott density in ZnO deduced from the experiments is 1.5×10^{18} cm^{-3}. In addition, previous work by Klingshirn *et al* leads to the conclusion that the ZnO excitonic Mott density is equal to 5×10^{17} cm^{-3} and displays a weak temperature dependence [16].

It thus appears that the reported values for GaN Mott transition are equal to or higher than those of ZnO. However the latter exhibits a larger excitonic binding energy in comparison with that of GaN (60 meV versus 25 meV). Furthermore, it should be noted that because of the GaN larger Bohr radius (4.2 nm for GaN versus 1.8 nm for ZnO), the excitonic Coulomb interaction screening with the increase of the excitation intensity should be more efficient in GaN than in ZnO. In view of these results, it can be concluded that the excitonic Mott density in bulk GaN needs to be revisited.

The Mott transition is found to be temperature dependent from experimental and theoretical points of view; this work is only focused on the analysis of GaN excitonic features at cryogenic temperatures as a function of the injected carrier density through micro-photoluminescence (μ-PL) and time resolved photoluminescence experiments (TRPL).

2. Experimental procedure

The sample is a 350 μm thick freestanding GaN layer, unintentionally doped, which has been grown by hydride vapor phase epitaxy. It is of high crystalline quality, with a dislocation density between 10^6 cm^{-2} and 10^7 cm^{-2} [17, 18].

The μ-PL experiments were carried out in a closed loop He cryostat at 5 K. The sample was investigated under a continuous wave excitation using an HeCd laser (325 nm) and a pulsed excitation using a Q-switched laser (266 nm). Given that the pulse duration (400 ps, repetition rate 20 kHz) is larger than the

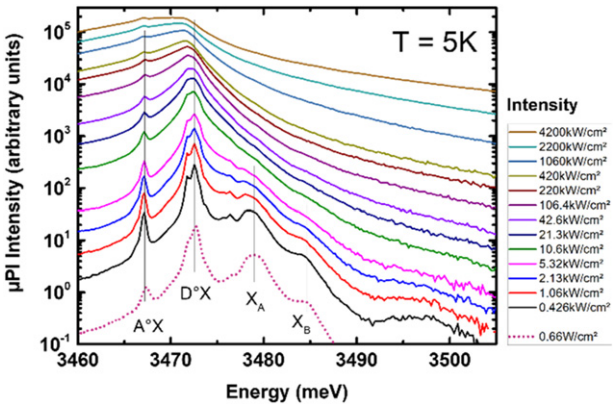


Figure 1. Photoluminescence spectra at 5 K of the free-standing GaN sample. The bottom dotted curve was measured with a HeCd laser (325 nm) for a power density of 0.66 W cm^{-2}. The solid curves were measured with a Q-switched laser (266 nm) for excitation intensities ranging from 0.42 kW cm^{-2} to 4200 kW cm^{-2}. The main peak corresponds to the recombination of an exciton bound to a neutral donor (D°X) at 3472.5 meV. The other optical transitions are identified as the recombination of excitons bound to neutral acceptors A°X at 3467.2 meV, of free excitons X_A and X_B at respectively 3478.5 meV and 3484.3 meV. At higher energy $X_A{}^{n=2}$ at 3497.5 meV is also detected.

measurements of the carrier lifetime, the excitation can be considered as a quasi-continuous wave excitation. The experimental setup consists of a confocal alignment with a microscope objective (10 mm focal length, 0.4 numerical aperture) used for both excitation and detection and a focal lens for detection and imaging through the spectrometer slits. The signal is then analyzed by a Jobin Hyvon HR1000 spectrometer equipped with a 1200 grooves/mm grating and detected by a 1024 × 256 pixels CCD (charged-coupled device) camera with a maximum resolution of 0.1 Å. In addition to the μ-PL experiments, TRPL were performed by means of a Ti:sapphire laser featuring 150 fs pulse duration and 76 MHz repetition rate. The laser frequency is tripled through non-linear crystals in order to obtain a wavelength of 266 nm. The luminescence decay is then dispersed by a spectrometer equipped with a 600 grooves mm^{-1} grating and temporally analyzed with a Hamamatsu streak camera; the time resolution of the set-up is about 7–8 ps.

Figure 1 displays μ-PL spectra measured at a cryogenic temperature of 5 K with continuous (HeCd laser) and quasi-continuous (Q-switched laser) excitations. Only one spectrum (purple curve at the bottom) recorded with the HeCd laser is reported in this figure; it corresponds to a weak excitation of 0.66 W cm^{-2}. Other spectra have been obtained with the Q-switched laser and excitation intensities were varying from 0.426 to 4200 kW cm^{-2}.

The main optical transitions are clearly identified at low excitation levels. The recombination of excitons bound to neutral acceptors A°X and neutral donors D°X are found at 3467.2 meV and 3472.5 meV respectively. The energies of the free exciton (X_A and X_B) recombinations (3478.5 meV and 3484.3 meV) indicate that no residual strain is present in the sample [19]. The first excited state of X_A exciton ($n = 2$) is also detected at higher energy (3497.5 meV).

As illustrated by the PL spectra in figure 1, the free-exciton lines progressively disappear with the increase of the excitation intensity and the D°X line peak shifts toward the low energy side. The redshift of the main luminescence peak (initially the D°X transition) is concomitant with the disappearance of the excitonic signature. Both features allow us to conclude that the Mott transition occurs for an excitation intensity between 10.6 and 21.2 kW cm^{-2}. The redshift evidences the bandgap renormalization with increasing carrier density. The energy of the bandgap decreases until the point where it passes below the energy of the excitons. This phenomenon occurs near the surface of the sample where the carrier density is the highest as it will be discussed in the following.

To ensure that the bandgap energy reduction followed with the redshift of D°X line actually comes from a density-dependent process induced by the optical excitation, electronic temperatures for excitation intensities below and above the vanishing of excitonic lines were extracted. Since for the lowest excitation intensities the electronic temperature (T_e) can not be extracted from the high-energy tail as commonly done [14], due to the presence of the free exciton emission, an alternative method has been employed. This method requires fitting the shape of the first excitonic X_A LO (longitudinal optical)-replica (not shown in this figure) by the following expression [20, 21]:

$$I_1^{\mathrm{lum}}(\hbar\omega) \propto E_{\mathrm{kin}}^{3/2} \exp\left(-\frac{E_{\mathrm{kin}}}{k_B T_e}\right) \quad (1)$$

with $\hbar\omega = E_{X_A} - \hbar\omega_{LO} + E_{kin}$ and where E_{X_A} is the energy of the X_A line, E_{kin} the excitonic kinetic energy and $\hbar\omega_{LO}$ the energy of the LO phonon.

The electronic temperature determines the distribution of off-equilibrium carriers, as given by Boltzmann's statistics [20]. Meanwhile, the crystal temperature (or lattice temperature) remains equal to 5 K, given the thermal exchange between the sample and its support. The variation of the bandgap with the lattice temperature is associated with the variation of the lattice parameters and of the population of phonons, but not with the electronic temperature.

The extracted electronic temperature remains near the cryostat temperature (5 K), as it is equal to 26–28 K for the first lowest excitation intensities obtained with the Q-switched laser. The electronic temperature increases to 32 K for an excitation intensity of 10.6 kW cm^{-2} where the free-exciton lines are no more distinguishable.

The red-shift of the D°X line is also a criterion which has been used previously by Binet *et al* to identify the Mott transition in GaN [14]. To do so the energy of D°X needs to be tracked as a function of the injected carried density, which has to be precisely evaluated. The carrier density corresponds to the total electron density and, thus, includes all species (i.e., electrons, donor and acceptor-bound excitons as well as free-excitons). In a general point of view, the carrier density is rather difficult to assess. Our experiments have been carried out with a bulk GaN sample and the luminescence signal comes mainly from the surface of the sample where the carrier density is the highest but the distribution of carriers throughout the sample is not homogeneous.

In our case, owing to the fact that the laser pulse duration is larger than the lifetime of the injected carriers, it is possible to calculate the carrier density n in the steady state regime [22, 23]. It supposed that the electron (n) and hole (p) densities remain equal (n = p) during the optical excitation.

The carrier density, if we neglect in-plane diffusion, is solution of the following 1D spatial- and time-dependent differential equation:

$$\frac{\partial n(x,t)}{\partial t} = \alpha\Phi\, e^{-\alpha x} + D\frac{\partial^2 n(x,t)}{\partial x^2} - \frac{n(x,t)}{\tau}. \tag{2}$$

Equation (2) is solved for the steady state (i.e. $\frac{\partial n(x,t)}{\partial t} = 0$) and the distribution of carrier density $n(x)$ in the depth is determined. This leads to the carrier density expression which corresponds to the carrier density at the sample surface, where the density is largest:

$$n(x=0) = \frac{\phi\tau}{\frac{1}{\alpha} + \sqrt{D\tau}} = \frac{I(1-R)\tau}{h\nu\left(\frac{1}{\alpha} + \sqrt{D\tau}\right)}, \tag{3}$$

where ϕ is the photon flux given by $\frac{I(1-R)}{h\nu}$, I is the excitation intensity, τ the carrier lifetime (which depends on the particle density), $h\nu$ the energy of the Q-switched laser, R the reflection coefficient, α the absorption coefficient at this energy and D the carrier diffusion coefficient. The values of these parameters are $(1-R) = 0.8$, $\alpha = 1.2 \times 10^5$ cm^{-1} and $D = 7$ cm^2 s^{-1} [24]. Surface recombination is not included in this calculation since it is taken into account implicitly through the carriers lifetime, which is measured experimentally. This procedure could overestimate carrier density as the lifetime measured is not negligible compared to the pulse duration.

3. Carrier density determination

TRPL experiments were performed at 5 K in order to assess the average carrier lifetime (τ) of the electron population, which is assumed to be equal to that of the holes. All radiative and non-radiative recombination channels are grouped in a mean lifetime which depends on carrier density. The τ value is obtained through a mono-exponential fit of the TRPL signal and is found to depend on the excitation intensity.

The electronic temperatures were measured with the TRPL setup by the same method presented for the quasi-continuous wave experiments and were found to be around 33 K. Since for the TRPL measurements the pulse duration ($t_p = 150$ fs) is shorter than the carrier lifetime, the corresponding injected carrier density can be estimated at the end of the pulse duration by the following equation:

$$n_{TRPL} = \frac{I_{TRPL} \times (1-R) \times t_p \times \alpha}{h\nu} \tag{4}$$

n_{TRPL} is identified with the carrier density n in equation (3) and will be associated to the lifetime τ deduced from the fitting of the PL decay with a single exponential function. By combining equation (3) with the experimental determination of $n(\tau)$ through the analysis of the TRPL data, it is possible to extract the carrier density as a function of excitation intensity I in the μ-PL experiments. A graphical approach

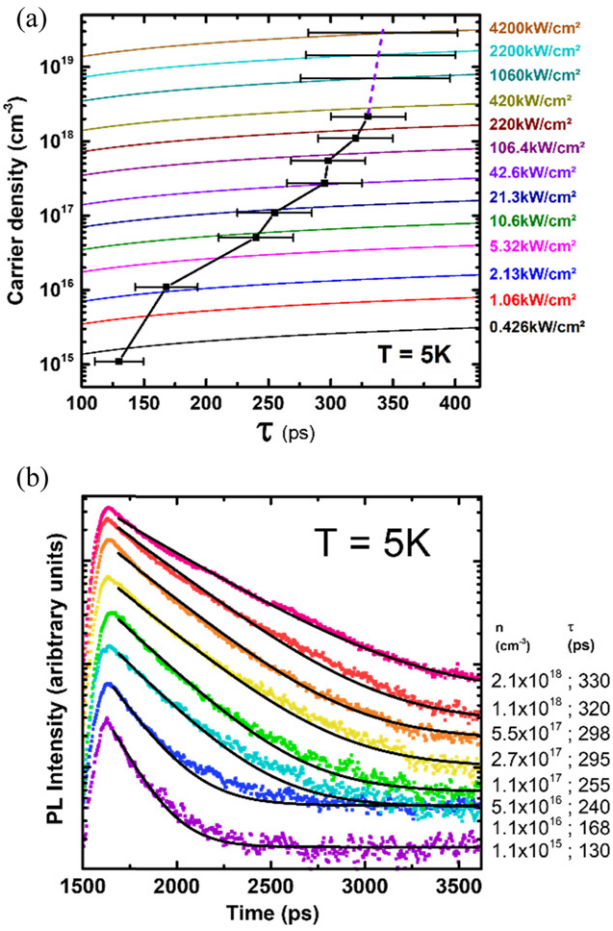


Figure 2. Experimental measurements of the carrier lifetime τ are reported as a function of carrier density n at 5 K. The use of equation (3) allows to calculate $n(\tau)$ for various excitation intensities. Intersection of these curves with the set of experimental data provides a correspondence between the carrier density and the excitation intensity. (a) Lifetimes extracted by applying mono-exponential fits to the time-resolved spectra of freestanding GaN at $T = 5$ K. (b) Mono-exponential PL decay fit at $T = 5$ K.

displayed in figure 2(a) is proposed to evaluate n as a function of I, where the experimental data $n_{\mathrm{TRPL}}(\tau) = n(\tau)$ are reported on the figure together with the evolution $n(\tau)$ for various excitation intensities I, as given by equation (3).

Figure 2(a) summarizes the results obtained thanks to the data analysis: τ corresponds to the decay time extracted by fitting the PL decay with a single exponential function, as shown in figure 2(b) and given by $y = y_0 + A\,\mathrm{e}^{-t/\tau}$.

It is important to note that in the figure 2(a), the carrier density displays a continuous dependence on carrier lifetime. It was not possible to measure the lifetime constant τ through TRPL experiments for high carrier densities owing to the limitation of the available excitation intensity (I_{TRPL}). Consequently, the three last τ values have been extrapolated as shown on figure 2(a).

The redshift of the D°X line as a function of the carrier density n is then reported in figure 3. This red-shift, which evidences the bandgap renormalization [25], is observed from a carrier concentration of 6×10^{16} cm^{-3}. Calculations of the excitonic fraction with respect to the whole amount of injected carriers are carried out within the model proposed by Versteegh *et al* [15].

The results are reported in figure 3 for a temperature of 30 K, which corresponds roughly to the measured electronic temperature. The theoretical Mott transition is evaluated to be about 8–9 $\times$ 10^{16} cm^{-3}, in good agreement with the experimental observations. As shown by the theoretical curve, this transition is not abrupt since it occurs between 3 $\times$ 10^{16} cm^{-3} and 9 $\times$ 10^{16} cm^{-3}. It is also worth noting that, as shown in figure 2(a), the carrier lifetime exhibits a value of 242 ps around the Mott transition.

To compute n_{Mott}, we use the approach developed by Versteegh *et al* [15], which considers the screening of the excitonic Coulomb interaction through the Yukawa potential [26] characterized by the screening length, λ_s within the approximation of static screening. This approximation has been verified in the case of GaN. The Mott density corresponds to the density at which λ_s is decreased to the exciton Bohr radius a_0. λ_s is derived using numerical calculation from the chemical potentials of electrons and holes as function of the

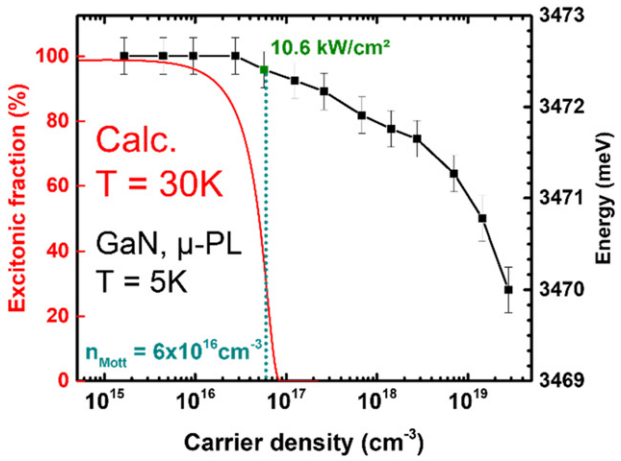


Figure 3. The energy of D°X is plotted as a function of the carrier concentration injected by optical excitation. The redshift of this transition from 10.6 kW cm^{-2} indicates the occurrence of the bandgap renormalization and coincides with the drop of the excitonic fraction. Those phenomenon implies that the Mott transition is occurring which corresponds to a carrier density of 6×10^{16} cm^{-3}. The Mott transition is not abrupt and is included in the 3×10^{16} cm^{-3}–9×10^{16} cm^{-3} range. The calculation of the excitonic fraction for a temperature of 30 K is found in good agreement with the experimental observation.

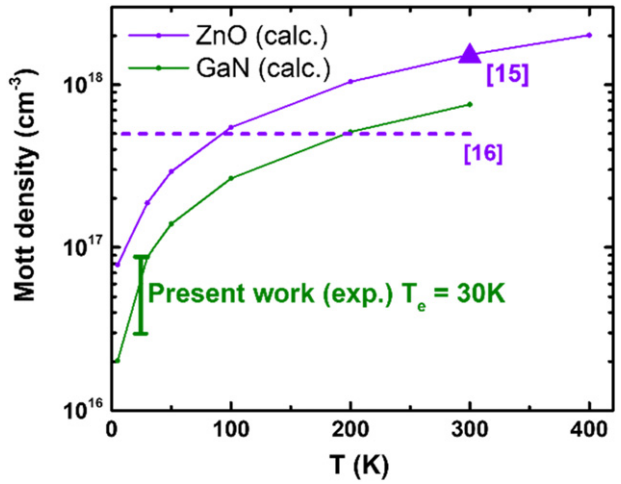


Figure 4. Theoretical and experimental values of the carrier density n_{Mott} at the excitonic Mott transition. The excitonic Mott transition are reported in the case of GaN and ZnO for comparison. n_{Mott} in GaN is necessarily lower than the one of ZnO owing to the difference of the excitonic binding energies of these materials (25 meV for GaN versus 60 meV for ZnO). Our experimental values for GaN are in good agreement with the calculations given by the model of Versteegh *et al* [15].

carrier density n in the ideal gas approximation. It only slightly overestimates the screening due to a weaker screening by excitons than by unbound carriers. In a self-coherent approach, the calculation can be refined by computing the excitonic fraction n_{ex}/n, which represents the fraction of carriers bound together to form excitons with respect to the total carrier density.

Figure 4 reports the theoretical evolution of the Mott density (n_{Mott}) calculated from the Versteegh model [15] for various temperatures in the case of GaN and ZnO. Experimental determinations of n_{Mott} reported in previous works are also indicated on figure 4 in the case of ZnO (5×10^{17} cm^{-3} temperature-independent [16], 1.5×10^{18} cm^{-3} $T = 300$ K [15]). If a scaling law is assumed between GaN and ZnO, it can be concluded that the n_{Mott} value for GaN is necessarily lower than that for ZnO. It is reminded here that the excitonic binding energy of ZnO is a factor 2.4 larger than that of GaN. The experimental value of the Mott density deduced from the present study is found to be in good agreement with the calculation for a temperature of 30 K.

4. Discussion

The Mott density determined in this work is more than one order of magnitude smaller than previous measurements and it is worth analyzing the possible origins of this discrepancy. Binet *et al* [14] have carefully analyzed the Mott transition in a bulk GaN sample through PL experiments as a function of power and temperature, i.e. under measurement conditions close to ours. The criterion which was used to detect the Mott transition is the red-shift of the emission line. At a bath temperature of 30 K they estimated a Mott density between 1.8 and 3.8 $\times$ 10^{18} cm^{-3}, with an electronic temperature of 120 K. The time dependence of the evolution of carrier density can be described through the following equation:

$$\frac{\mathrm{d}n\,(t)}{\mathrm{d}t} = G - \frac{n}{\tau_\mathrm{r}} - \frac{n}{\tau_\mathrm{nr}} - \beta_\mathrm{r} n^2 - \beta_\mathrm{nr} n^2 \tag{5}$$

with G the generation term, τ_r and τ_nr respectively the radiative and non radiative recombination times, β_r, β_nr the radiative and non radiative bimolecular recombination coefficients [22].

The evaluation of the injected carrier density has to be necessarily carried out by considering simultaneously the two following phenomena: the monomolecular and bi-molecular recombinations, the former being crucial particularly in the case of short carrier lifetimes. Note that this explains why one cannot directly compare excitation intensities when discussing Mott density, as the actual carrier densities for a given excitation intensity depend crucially on the carrier lifetime, which can be one order of magnitude different depending on the sample. Compared to ours, in Binet's work [14] the carrier density is evaluated by assuming only a bi-molecular recombination, while the mono-molecular term associated to a certain carrier lifetime is neglected. The use of the bi-molecular term $-\beta n^2$ (with $\beta = \beta_\mathrm{r} + \beta_\mathrm{nr} = 1.3 \times 10^{-8}$ cm^3 s^{-1}, n is the carrier density) instead of the mono-molecular one, $-n/\tau$, overestimates for short lifetimes, the evaluation of the carrier density n from the measurement of the excitation intensity [22]. Besides, the high electronic temperature with respect to the bath temperature reported by the authors suggests a short carrier lifetime. In this case a high excitation intensity is needed to maintain a sufficiently high carrier concentration so as to detect the Mott transition. If we assumed a monomolecular recombination, it is necessary to consider a lifetime of about 26 ps to match our theoretical estimation of $n_\mathrm{Mott} = 4.0 \times 10^{17}$ cm^{-3} for an electronic temperature of 123 K with a 314 kW cm^{-2} power excitation, as used in [14]. Interestingly, carrier lifetimes measured by TRPL in similar samples as those employed by Binet and co-workers displayed values in the order of 24 ps at these temperatures [31], consistent with our estimations. It is worth comparing the contributions of bi-molecular and mono-molecular recombinations in the present work at the Mott transition, for $n = 6 \times 10^{16}$ cm^{-3}. The mono-molecular term is found to be larger than the bi-molecular one by a factor 5.1, thus showing that the bi-molecular term can be neglected.

Auger recombination could be also considered for evaluating the injected photo-carriers; to do so the term $-Cn^3$ has to be included in the right part of equation (5) of the manuscript. However, the calculation of this term for carrier densities lying in the investigated range in our experiments leads to the conclusion that this quantity can be disregarded with respect to the mono- and bi-molecular recombinations. Indeed, its absolute value is roughly five orders of magnitude smaller than the other two terms (for the current carrier densities). The C value used in the calculation is extracted from reference [32].

Moreover, the determination of the carrier lifetime through TRPL experiments (assuming a mono-exponential decay) accounts for the small contribution of the bi-molecular term, since the fitting procedure provides an effective recombination time corresponding to the measured carrier density.

Fisher's work reports another detailed analysis of the screening of excitons in a GaN slab through femtosecond pump-probe absorption [13]. Absorption spectra are measured at 5 K for various excitations intensities. The authors underline in this paper that the absorption of the pump is not homogeneous since the GaN thickness is equal to 0.38 μm while the absorption length at the laser energy is considered equal to 0.11 μm.

Consequently, the Mott density can be reached at the illuminated front face of the sample while excitons remain present at the back side. Our sample also behaves as a semi-infinite system in which the distribution of carriers is necessarily inhomogeneous and, as discussed already, in a quasi-stationary regime it is possible to determine the distribution of carriers (electrons, n) as a function of the depth x of the sample. This distribution can be written, neglecting in-plane carrier diffusion and without considering surface recombination, as:

$$n\,(x) = \frac{\phi\alpha\tau}{1-\alpha^2 L^2}\left(\mathrm{e}^{-\alpha x} - \alpha L\,\mathrm{e}^{-\frac{x}{L}}\right) \tag{6}$$

with $L = \sqrt{(D\tau)}$.

Compared to our PL experiments, in this experimental configuration (pump-probe absorption) it is very difficult to estimate reliable carrier densities as both the inhomogeneous spreading of carriers and the

Table 2. Summary of exciton binding energy and Mott densities at low temperature ($T < 25$ K) for wide bandgap semiconductors. The value corresponding to GaAs is also reported.

	CuCl [27]	Cu_2O [28]	ZnO [15]	CdS [29]	GaN[a]	GaAs [30]
E_b (meV)	190	150	60	29	25	4.2
n_{Mott} (cm^{-3})	5×10^{19}	3×10^{18}	1.5×10^{17}	5×10^{16}	6×10^{16}	7×10^{15}

[a]This work.

variable screening of excitons along the sample have to be considered, which requires time- and spatial-dependent simulations. Indeed, Fisher *et al* reported a Mott density of 1×10^{18} cm^{-3} without indicating precisely the way they followed to estimate it.

Reported values of the excitonic Mott density at low temperature (<25 K) in other wide gap semi-conductors are listed in table 2, the value corresponding to GaAs is also reported for information.

5. Conclusion

In conclusion, photoluminescence experiments carried out at 5 K under a quasi-continuous excitation have evidenced the Mott transition in GaN through the bleaching of excitons and the bandgap renormalization.

TRPL allowed to correlate the excitation intensity with the injected carrier density. The Mott transition in bulk GaN is found to occur for a carrier density equal to $(6 \pm 3) \times 10^{16}$ cm^{-3}, in accordance with theoretical calculations considering an electronic temperature of 30 K. This new determination will enable to analyze in detail the role of excitons in GaN-based photonic devices operating in the high-injection regime.

Acknowledgments

We acknowledge support from GANEXT (ANR-11-LABX-0014); GANEXT belongs to the publicly funded 'Investissements d'Avenir' program managed by the Agence Nationale de la Recherche (ANR), France. We also thanks Dr Jean-Yves Duboz from CRHEA for insightful discussions and Dr Bernard Beaumont from Lumilog for providing the high quality sample.

Data availability statement

The data that support the findings of this study are available upon reasonable request from the authors.

ORCID iDs

Léo Mallet-Dida https://orcid.org/0000-0001-7896-8589

References

[1] Pattison P M, Hansen M and Tsao J Y 2018 LED lighting efficacy: status and directions *C. R. Phys.* **19** 134
[2] Mallet E, Réveret F, Disseix P, Shubina T V and Leymarie J 2014 Influence of excitonic oscillator strengths on the optical properties of GaN and ZnO *Phys. Rev.* B **90** 045204
[3] Zúñiga-Pérez J *et al* 2016 Polarity in GaN and ZnO: theory, measurement, growth, and devices *Appl. Phys. Rev.* **3** 041303
[4] Imamoglu A, Ram R J, Pau S and Yamamoto Y 1996 Nonequilibrium condensates and lasers without inversion: exciton–polariton lasers *Phys. Rev.* A **53** 4250
[5] Bajoni D 2012 Polariton lasers. Hybrid light–matter lasers without inversion *J. Phys. D: Appl. Phys.* **45** 313001
[6] Hönerlage B, Klingshirn C and Grun J B 1976 Spontaneous emission due to exciton–electron scattering in semiconductors *Phys. Status Solidi b* **78** 599
[7] Mohs G, Aoki T, Shimano R, Kuwata-Gonokami M and Nakamura S 1998 On the gain mechanism in GaN based laser diodes *Solid State Commun.* **108** 105
[8] Alemu A, Gil B, Julier M and Nakamura S 1998 Optical properties of wurtzite GaN epilayers grown on *A*-plane sapphire *Phys. Rev.* B **57** 3761
[9] Versteegh M A M, Vanmaekelbergh D and Dijkhuis J I 2012 Room-temperature laser emission of ZnO nanowires explained by many-body theory *Phys. Rev. Lett.* **108** 157402
[10] Gay J G 1971 Screening of excitons in semiconductors *Phys. Rev.* B **4** 2567
[11] Hess S, Taylor R A, Kyhm K, Ryan J F, Beaumont B and Gibart P 1999 Femtosecond exciton dynamics and the Mott transition in GaN under resonant excitation *Phys. Status Solidi b* **216** 57

[12] Kyhm K, Taylor R A, Ryan J F, Beaumont B and Gibart P 2004 Electron–hole plasma Mott transition and stimulated emission in GaN *J. Korean Phys. Soc.* **45** 526
[13] Fischer A J, Little B D, Schmidt T J, Choi C-K, Song J-J, Horning R D and Goldenberg B L 1999 Ultrafast carrier dynamics in GaN epilayers studied by femtosecond pump-probe spectroscopy *Ultrafast Phenomena in Semiconductors III* (Optoelectronics '99 - Integrated Optoelectronic Devices, 1999, San Jose, CA, United States 1999) vol 3624 ed K-T F Tsen pp 179–87
[14] Binet F, Duboz J Y, Off J and Scholz F 1999 High-excitation photoluminescence in GaN: hot-carrier effects and the Mott transition *Phys. Rev.* B **60** 4715
[15] Versteegh M A M, Kuis T, Stoof H T C and Dijkhuis J I 2011 Ultrafast screening and carrier dynamics in ZnO: theory and experiment *Phys. Rev.* B **84** 035207
[16] Klingshirn C, Hauschild R, Fallert J and Kalt H 2007 Room-temperature stimulated emission of ZnO: alternatives to excitonic lasing *Phys. Rev.* B **75** 115203
[17] Gogova D *et al* 2005 High-quality 2″ bulk-like free-standing GaN grown by hydride vapour phase epitaxy on a Si-doped metal organic vapour phase epitaxial GaN template with an ultra low dislocation density *Japan. J. Appl. Phys.* **44** 1181
[18] Aoudé O, Disseix P, Leymarie J, Vasson A, Aujol E, Beaumont B, Trassoudaine A and André Y 2006 Continuous wave and ultra-fast reflectivity studies for the determination of GaN excitonic oscillator strengths as a function of the in-plane biaxial strain *Superlattices Microstruct.* **40** 166
[19] Monemar B, Paskov P P, Bergman J P, Toropov A A, Shubina T V, Malinauskas T and Usui A 2008 Recombination of free and bound excitons in GaN *Phys. Status Solidi b* **245** 1723
[20] Klingshirn C F 2012 *Semiconductor Optics* 4th edn (Berlin: Springer)
[21] Hauschild R, Priller H, Decker M, Brückner J, Kalt H and Klingshirn C 2006 Temperature dependent band gap and homogeneous line broadening of the exciton emission in ZnO *Phys. Status Solidi c* **3** 976
[22] Pelant I and Valenta J 2012 *Luminescence Spectroscopy of Semiconductors* (Oxford: Oxford University Press)
[23] Mathieu H and Fanet H 2009 *Physique Des Semiconducteurs et Des Composants Électroniques—6ème Édition: Cours et Exercices Corrigés* 6th edn (Paris: Dunod)
[24] Netzel C, Hoffmann V, Tomm J W, Mahler F, Einfeldt S and Weyers M 2020 Temperature-dependent charge carrier diffusion in $[000\bar{1}]$ direction of GaN determined by luminescence evaluation of buried InGaN quantum wells *Phys. Status Solidi b* **257** 2000016
[25] Haug H and Schmitt-Rink S 1985 Basic mechanisms of the optical nonlinearities of semiconductors near the band edge *J. Opt. Soc. Am.* B **2** 1135
[26] Snoke D 2008 Predicting the ionization threshold for carriers in excited semiconductors *Solid State Commun.* **146** 73
[27] Nagai M, Shimano R and Kuwata-Gonokami M 2000 Direct creation of electron–hole plasma by exciton Mott transition in CuCl *J. Lumin.* **87–89** 192
[28] Manzke G, Semkat D, Richter F, Kremp D and Henneberger K 2010 Mott transition versus Bose–Einstein condensation of excitons *J. Phys.: Conf. Ser.* **210** 012020
[29] Egorov V D, Müller G O, Zimmermann R, Dite A F, Lysenko V G and Timofeev V B 1981 Photoconductivity of CdS under high excitation—indicating no homogeneous Mott transition *Solid State Commun.* **38** 271
[30] Shah J, Leheny R F and Wiegmann W 1977 Low-temperature absorption spectrum in GaAs in the presence of optical pumping *Phys. Rev.* B **16** 1577
[31] Im J S, Moritz A, Steuber F, Härle V, Scholz F and Hangleiter A 1997 Radiative carrier lifetime, momentum matrix element, and hole effective mass in GaN *Appl. Phys. Lett.* **70** 631
[32] Kioupakis E, Yan Q, Steiauf D and Van de Walle C G 2013 Temperature and carrier-density dependence of auger and radiative recombination in nitride optoelectronic devices *New J. Phys.* **15** 125006